THE JOURNAL OF PHYSICAL CHEMISTRY A

ARTICLE

pubs.acs.org/JPCA

Electronic States of the Benzene Dimer: A Simple Case of Complexity

Kadir Diri and Anna I. Krylov*

Department of Chemistry, University of Southern California, Los Angeles, California 90089-0482, United States

Supporting Information

ABSTRACT: Electronic structure calculations of the excited states of the benzene dimer using equation-of-motion coupled-cluster method are reported. The calculations reveal large density of electronic states, including multiple valence, Rydberg, and mixed Rydberg-valence states. The calculations of the oscillator strengths for the transitions between the excimer state (i.e., the lowest excited state of the dimer, 1^1B_{1g}) and other excited states allowed us to identify the target state responsible for the excimer absorption as the E_{1u} state of a mixed Rydberg-valence character at 3.04 eV above the excimer (1^1B_{1g}). Although at D_{6h} the $1^1B_{1g} \rightarrow E_{1u}$ transition is symmetry-forbidden, small geometric displacements (to D_{2h}) that have a negligible effect on the excitation energy split this degenerate state into the dark ($4B_{3u}$) and bright ($4B_{2u}$) components (oscillator strength of 0.3 au). The excitation energy for this transition depends strongly on the dimer structure, which explains the broad character of the experimentally observed excimer absorption spectrum.

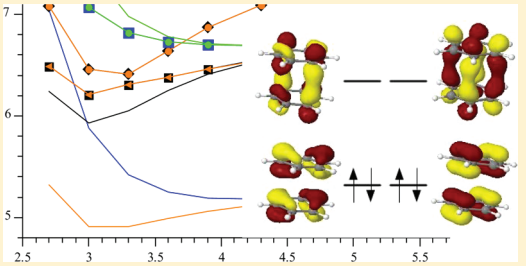

1. INTRODUCTION

Initially, the term "excimer" (short for excited dimer) was coined to describe a dimer that is bound only in the electronically excited state(s) and is, therefore, a short-lived species. Fluorescence from excimers usually results in broad and structureless peaks, in agreement with repulsive ground state potential energy surfaces (PESs). Strictly speaking, excimers do not have purely repulsive ground-state PESs, but are weakly bound in the ground state, in contrast to a much stronger binding energy (and shorter interfragment distance) in the excited state. For example, the binding energy (D_0) of the benzene dimer is about 2.6 kcal/mol,[1] whereas its first excited state is bound by about 8.1 kcal/mol.[2,3]

The first excimer that was identified was the triplet-state excimer of the mercury dimer.[4] The first reported singlet excimer was that of helium.[5,6] Excimers of other noble gases have been subsequently observed[7] and even though they did not attract much attention initially, they have led to important technological applications such as excimer lasers.

Excimer formation has been observed not only in gases, but also in solutions, pure liquids, photodimerization processes, single crystals, and defects in crystals.[7] Intramolecular excimer fluorescence has also been observed in aromatic polymers[8] and dinucleotides.[9] The thymine excimer is especially important as the precursor of the thymine photodimer, which is involved in the radiative damage of DNA.[7,10,11]

Aromatic excimers (AE) were first noted by Förster and Kasper in the fluorescence spectrum of pyrene.[12] AE formation in fluid solutions is now considered a rule rather than an exception.[7] The benzene dimer is of particular interest as the simplest prototypical AE for which accurate calculations can be performed, to compliment the abundance of data generated in numerous experimental studies.[7,13−21]

The mechanism of formation of the benzene excimer (BE), the nature of its electronic states, and the absorption mechanism have generated some controversy. For instance, the traditional view of the excimer being formed by the interaction of a monomer in its ground state with a monomer in an excited state[13] has been challenged by more recent experiments where excitation to the S_1 monomer state leads to the formation of a van der Waals S_1 complex separated by a barrier from the lowest excimer (S_1) state.[22] Instead, the latter is obtained by exciting the monomer to the S_2 state, which first produces the S_2 van der Waals complex, which in turn undergoes internal conversion to the excimer's S_1 state.

The BE absorption, namely, a characteristic low-energy band at 2.4−2.5 eV, has also generated discussions. Similar near-IR absorption spectra have been observed in other aromatic excimers.[23] Birks assigned the absorption to the $B_{1g} \rightarrow E_{1u}$ excimer transition,[24] however, this assignment has been questioned by other studies[13,14,25] on the grounds that it is not consistent with the observed large absorption cross section, as it is forbidden from a group-theoretical perspective. This gave rise to alternative explanations, such as the geometry of the excimer not being D_{6h},[25] or assigning the transition from the B_{1g} state to the charge-transfer (i.e., ion-pair like) state that correlates to $(C_6H_6)^+ + (C_6H_6)^-$ (which is supported by the absence of a fluorescence signal coming from the neutral monomer following photoexcitation at 500 nm).[14] Another explanation that has been proposed is a possible symmetry-allowed transition to a state of E_{2u} symmetry,[13] however, the existence of such a state has not been supported by theory,[26] including this work.

Received: September 23, 2011
Revised: November 19, 2011
Published: November 21, 2011

The bonding in an excimer can be explained in terms of two stabilizing molecular interactions:[7] exciton resonance ($MM^* + M^*M$) and charge resonance ($M^-M^+ + M^+M^-$). In the framework of valence-bond theory, the former is similar to the so-called covalent contributions to a wave function, whereas the latter represents ionic terms (note that the presence of ionic configurations in the wave function does not imply asymmetric charge distribution leading to a permanent dipole moment). Studies of large AEs have accounted for the nature of the observed states in terms of exciton theory and, in some cases, in terms of charge resonance stabilized states; however, in many cases, neither of these simplified models can account for the observed results, and mixing of the two types of configurations provides a better description. This more accurate picture arises naturally from the excimer theory developed by East and Lim[27] for the naphthalene dimer and applied to other systems, such as the NO dimer.[28] A Similar analysis has been applied to describe the excited[29] and ionized[30,31] states of nucleobase dimers. In the case of BE, the source of stabilization of the excimer has been widely debated. Birks[32] suggested that the dominant stabilization is of charge-resonance type, while Vala et al.[26] concluded that the BE stability can be explained via the interaction of an exciton-resonance state with a charge transfer state at a higher energy. More recent experiments argue that the BE is primarily of charge transfer character.[14,15]

BE has been studied using extended Hückel[33] and semiempirical methods,[26,34] as well as time-dependent density functional theory[35] and high-level electronic structure methods, such as complete active space self-consistent field (CASSCF) and CASPT2 (perturbatively corrected CASSCF).[36] Various spectroscopically relevant properties, such as fluorescence, absorption, and binding energy, have also been obtained with a hierarchy of coupled cluster methods such as CC2, EOM-EE-CCSD (equation-of-motion coupled-cluster method for excitation energies with single and double substitutions), and CCSDR(3) (EOM-EE-CCSD with a perturbative triples correction).[37] The focus of the present study is on the complexity of the excited states manifold, which involves multiple interacting Rydberg and valence states, and the origin of the excimer absorption.

We employ EOM-EE-CCSD, which is a method of choice for this type of phenomena, as it is capable of providing a balanced description of Rydberg and valence states as well as electronic near and exact degeneracies[38] originating from the transitions between the degenerate pairs of MOs and giving rise to multiple Jahn−Teller manifolds.[39,40]

We characterize vertical state ordering and oscillator strengths of the ground-state benzene dimer and describe the correlation of the dimer states with those of the monomer. We then consider electronic absorption of the excimer, and assign the nature of the bright transition to the $B_{1g} \rightarrow E_{1u}$ state that gains considerable oscillator strength ($\approx$ 0.3 au) at very small symmetry-lowering displacements. In addition, we also characterize the excimer states at the equilibrium geometry of the benzene dimer cation,[41] as a possible route of excimer generation in the gas phase via a charge-exchange reaction between, for example, the benzene dimer cation and Cs.[42,43] Moreover, the structure of the excimer has been thought to be similar to that of the corresponding cation based on the higher two-color photoionization cross section (via the S_1 state) for the benzene dimer compared to the trimer.[16]

2. COMPUTATIONAL DETAILS

The structures of the monomers were frozen in all calculations using the CCSD(T)/cc-pVQZ geometry.[44] We considered the following structures of the dimer: (i) ground-state parallel-displaced sandwich (C_{2h});[1] (ii) slightly distorted (see below) parallel sandwich (D_{6h}) equilibrium structure of the excimer (that is, the lowest excited state of the sandwiched dimer, 1^1B_{1g});[36] and (iii) equilibrium structure of the dimer cation, x-displaced sandwich (C_{2h}).[41] In the calculation of absorption spectra, including the one for the monomer, all the D_{6h} structures were slightly distorted to a lower (D_{2h}) symmetry to assess the effect of symmetry lowering on the oscillator strengths. The equilibrium distances (R) between the planes of the fragments at the neutral and the cation ground states are 3.60 and 3.10 Å, respectively.[1,41] The distance between the monomers in the sandwich excimer was set to 3.05 Å, as reported by Rocha-Rinza et al.[36] The one-dimensional PES scans using EOM-EE yield a very similar equilibrium distance. In addition, we performed unconstrained EOM-EE optimization of the lowest excimer state starting from the ground state cation structure (C_{2h}). The optimization converges to the sandwich (D_{6h}) structure with a slightly longer interfragment distance of 3.15 Å. The latter is very close to the value obtained by Amicangelo from the potential energy scan of the lowest excimer state using TDDFT (time-dependent density functional theory) with the 6-31+G(d) basis set.[35] To summarize the differences between the three structures, (i) the interfragment distance is the largest in the ground-state neutral (3.60 Å) and is very similar in the excimer and the cation (3.05−3.10 Å); (ii) the symmetry of the neutral and the cation structure is C_{2h} (parallel-displaced sandwich), whereas the optimized excimer structure is D_{6h}.

We perform oscillator strength calculations at slightly distorted geometries of the monomer and excimer in order to assess the effect of symmetry lowering on the oscillator strengths. In the monomer this was done by elongating the bond lengths of two symmetric hydrogens by 0.001 Å, while in the dimer, the symmetry was broken by manipulating four hydrogens lying in a plane, including the main symmetry axis. Those hydrogens were displaced such that they get closer to the horizontal plane (σ_h) by 0.001 Å, which corresponds to an angle of about 0.1° away from the planes of the respective monomers. Thus, oscillator strengths shown below for the excimer and the monomer correspond to the distorted D_{2h} structure. Although the distortion has a negligible effect on the excitation energies (less than 0.003 eV in the monomer and less than 0.0003 eV in the sandwich dimer), it is important for intensities, for example, the optically dark $B_{1g} \rightarrow E_{1u}$ transition splits into optically dark and very bright transitions.

The electronic spectra were computed by EOM-EE-CCSD.[38,45] The core electrons were frozen. Most excited state calculations have employed the 6-31+G(d) basis set, which is similar in quality to aug-cc-pVDZ used in ref 37. This basis set is not sufficiently large for obtaining converged excitation energies and properties; however, it is capable of providing a semiquantitative picture of the excited state manifold, in particular, of the mixing between Rydberg and valence states.

To test the effect of a larger basis set on the sandwich dimer excitation energies, we calculated 16 states (two in each symmetry, which samples a mix of valence and Rydberg states) using the 6-311++G(d,p) basis set. We note that expanding the basis set affects primarily the Rydberg states, lowering their excitation

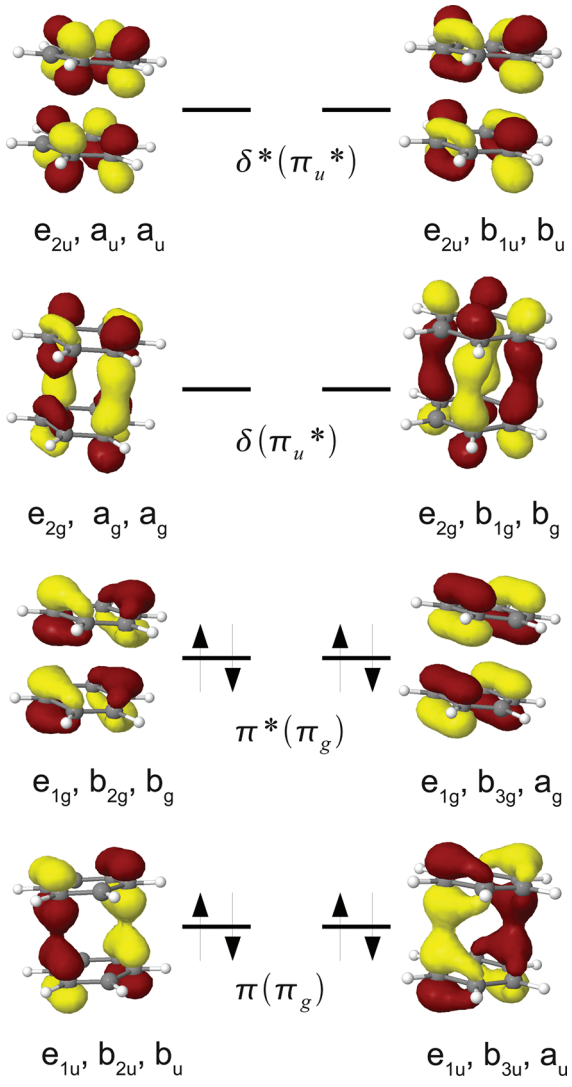

Figure 1. Relevant molecular orbitals of the sandwich-shaped benzene dimer computed with the 6-31G(d) basis set at the excimer's equilibrium geometry. Orbital symmetry labels "*x*, *y*, *z*" correspond to the D_{6h}, D_{2h}, and C_{2h} point groups, respectively. An isosurface value of 0.05 was used for the plot.

energies by up to 0.26 eV, while the effect on the valence states is smaller (up to 0.12 eV), as expected. A similar trend was observed in the *x*-displaced sandwich structure.

The monomer absorption spectrum was also calculated using the 6-311++G(d,p) basis set. We found that the excited state energies are affected by, at most, 0.36 eV, while the oscillator strengths are affected by, at most, 0.02, relative to the smaller 6-31+G(d) basis set. These calculations provide an estimate of the limitations of using the 6-31+G(d) basis set.

The potential energy scans of the sandwich dimer were done by varying the equilibrium distance *R* while keeping the monomers rigid. The reported energies were recalculated with respect to the ground-state dimer dissociation limit; i.e., the zero for the energy was set to the total energy of the dimer at 6.0 Å monomer separation. Most of the state energies at that separation have not reached their asymptotic limit, however, because the focus of this study is not on calculating accurate binding energies, this is not important.

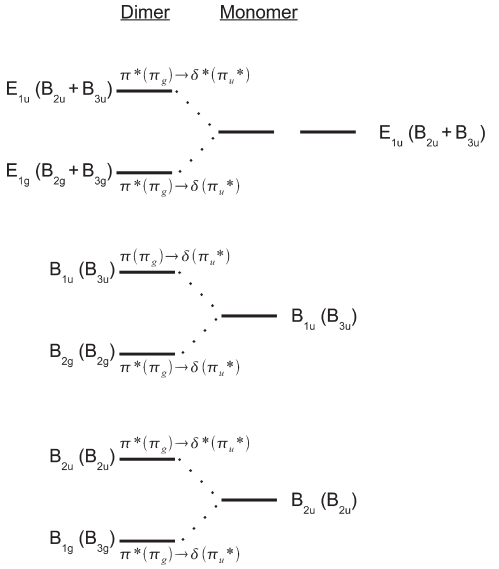

Figure 2. Diagram illustrating the correlation between the electronic states of the benzene dimer (left) and the levels of a ground state benzene monomer interacting with a monomer in its excited states (right). Labels in parentheses are for the D_{2h} point group.

Relevant Cartesian geometries, energies, and oscillator strengths are given in the Supporting Information. All calculations were performed using Q-Chem.[46]

3. RESULTS AND DISCUSSION

3.1. Molecular Orbital Framework. Figure 1 shows the two highest occupied and the two lowest unoccupied π molecular orbitals (MOs) of the sandwich-shaped benzene dimer. These orbitals are derived from in-phase and out-of-phase combinations of the benzene monomer's frontier orbitals. We labeled these according to the DMO-LCMO (dimer molecular orbital—linear combination of fragment molecular orbitals) scheme developed in a previous study of the benzene dimer cation[41] and later extended to ionized dimers of nucleobases.[30,31] That is, the labels of the dimer orbitals are given as $x(y)$, "*x*" being the overall symmetry (i.e., π, δ, etc.) of the MO with respect to the axis connecting the two monomers and "*y*" being the symmetry of the constituent monomer orbital.

We begin the discussion by considering a simple picture where a monomer in its ground state interacts with a monomer in an excited state to form a sandwich-shaped excimer (Figure 2) with D_{6h} symmetry. The lowest three states derived from the HOMO—LUMO transitions in the benzene monomer are B_{2u} (B_{2u}), B_{1u} (B_{3u}), and E_{1u} (B_{2u} + B_{3u}), respectively, where in parentheses we include the corresponding state symmetries in the D_{2h} point group (further on, we will utilize this point group since most electronic structure codes work with Abelian groups).

A monomer in its ground electronic state, interacting with another monomer in its lowest excited state, B_{2u} (B_{2u}), should give rise to two excimer states of symmetries B_{1g} (B_{3g}) and B_{2u} (B_{2u}).[36] The lowest calculated excited state (at 5.25 eV, see Figure 3a) of the monomer is symmetry-forbidden, however, it gives rise to experimentally observed absorption at 4.90 eV[47,48] owing to intensity borrowing facilitated by vibronic interactions. Such intensity borrowing could, in principle, make the lowest excimer state optically accessible, even though it is also

dx.doi.org/10.1021/jp209190e |J. Phys. Chem. A 2012, 116, 653–662

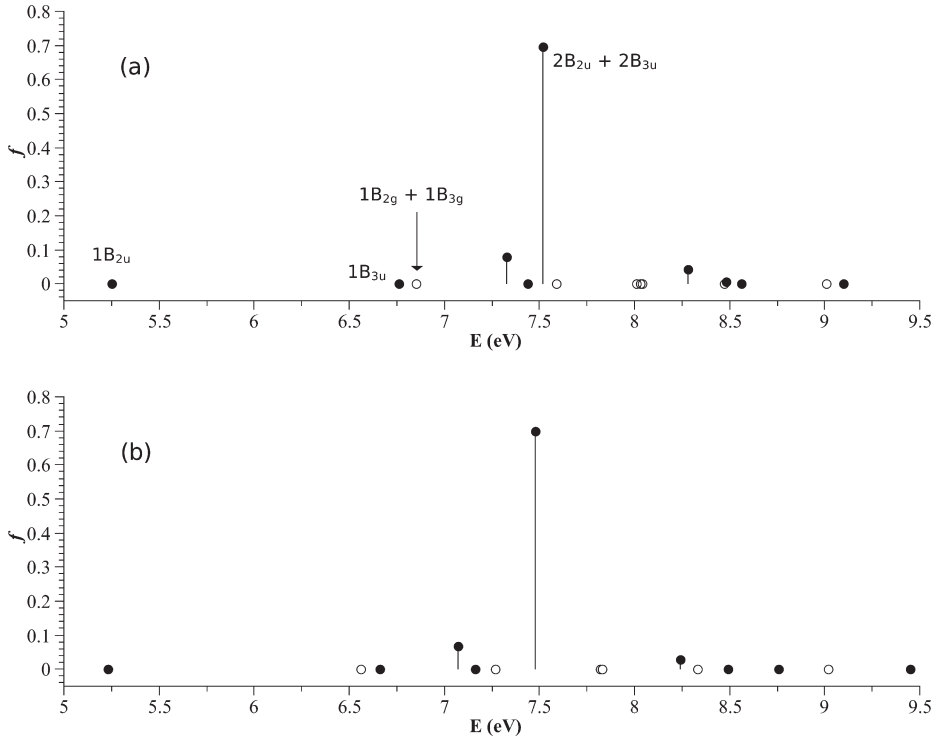

Figure 3. Absorption stick spectrum of the benzene monomer computed by EOM-EE-CCSD using the (a) 6-31+G(d) and (b) 6-311++G(d,p) basis sets. Empty circles show symmetry-forbidden transitions, while the full circles denote the allowed ones in the D_{2h} point group. In the D_{6h} point group, some of these transitions become forbidden, including the lowest two states.

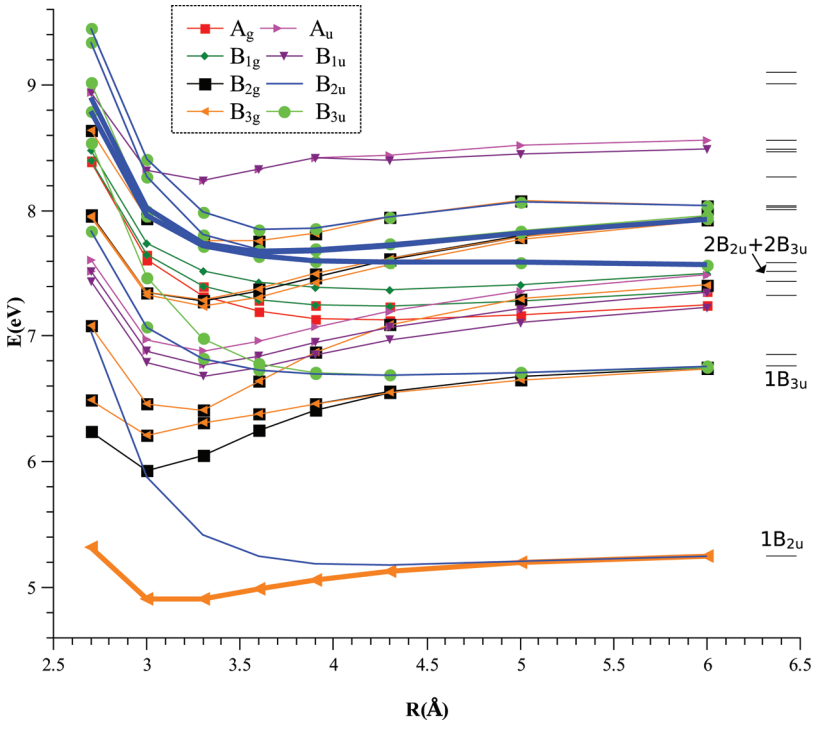

Figure 4. PES scan of the benzene excimer states along the interfragment distance. Shown on the right are the monomer energy levels along with the labels of the relevant states discussed in the text. D_{2h} point group labels were used in the plot.

symmetry-forbidden. Despite the fact that there is a consensus about the sandwich-shaped structure of the excimer, understanding the formation of this state has proven to be a more elusive issue. In optical absorption spectra of benzene S_1 in supersonic molecular jet, Law et al. argue in favor of barrierless excimer formation following the excitation of a parallel displaced

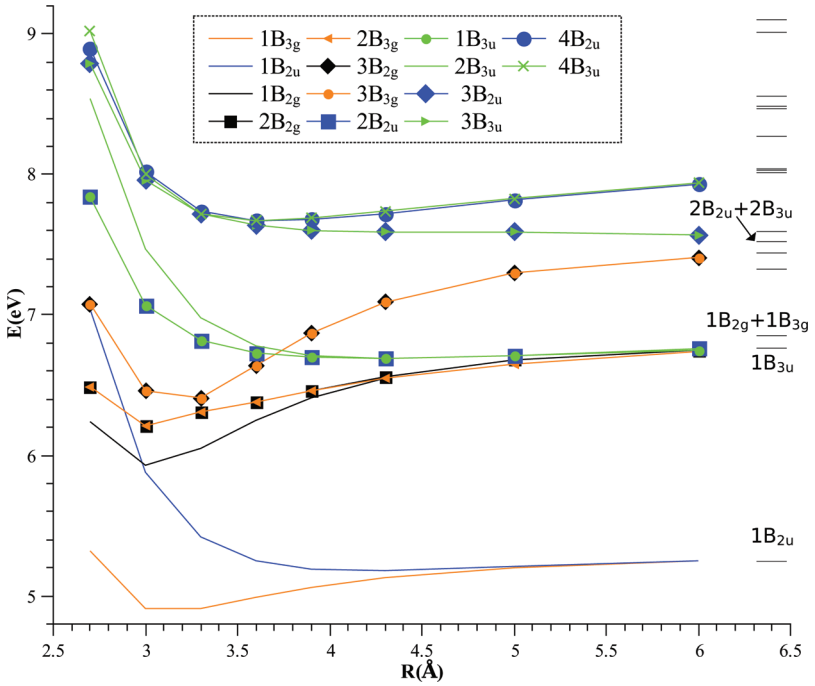

Figure 5. PES scan of relevant benzene excimer states along the interfragment distance. Shown on the right are the monomer energy levels along with the labels of the relevant states discussed in the text. D_{2h} point group labels were used in the plot.

ground-state dimer.[17] In similar experiments, Hopkins et al. attribute their results to the rearrangement of a T-shaped ground state dimer to a sandwich excimer structure within several picoseconds following the excitation.[16] The activation energy for this process was found to be 0.11 eV experimentally,[49] whereas calculations predict a much smaller barrier of 0.02 eV.[36] More recent experiments monitored the dynamics of the rearrangement of a T-shaped structure into a sandwich one, which occurs via tunneling through an energy barrier.[14] In two-color resonance-enhanced two-photon ionization experiments, Shinohara et al. obtained the lowest excimer state after excitation to S_2, which proceeds through an intermediate van der Waals S_2 state undergoing internal conversion to the excimer S_1 state, whereas an original excitation to S_1 does not necessarily produce the S_1 excimer state.[22] Instead, the latter excitation leads to the formation of the excited van der Waals S_1 state.

The second dimer state in Figure 2, B_{2u} (B_{2u}), derived from the interaction of a ground-state monomer with the monomer in its lowest excited state, is repulsive, in agreement with previous calculations.[35−37]

The second set of excimer states in Figure 2, that is, B_{2g} (B_{2g}) and B_{1u} (B_{3u}), results from the interaction of a ground state monomer with a monomer in its second excited state, that is, B_{1u} (B_{3u}). This monomer state is also symmetry-forbidden and the observation of the resulting excimer states has been a subject of debate. These excimer states have been omitted in previous theoretical studies[36,37] on the grounds that they have not been observed experimentally, although Shinohara and Nishi reported the lifetime of the benzene dimer S_2 state.[22] However, subsequent studies failed to reproduce these results.[50,51]

The third set of excimer states E_{1g} (B_{2g} + B_{3g}) and E_{1u} (B_{2u} + B_{3u}) are derived from a ground-state monomer interacting with a monomer in its excited E_{1u} (B_{2u} + B_{3u}) state. The latter state is symmetry-allowed and shows a strong absorption band at

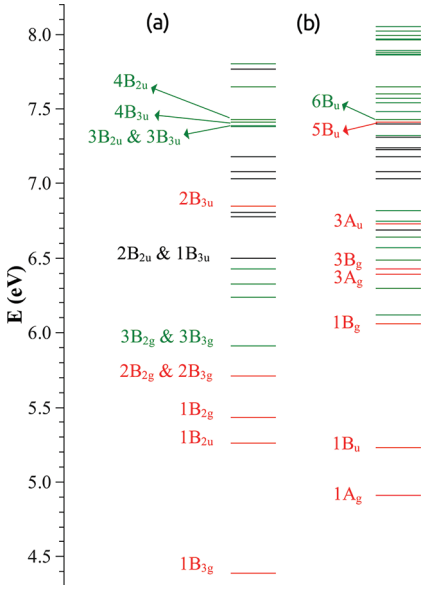

Figure 6. Rydberg (black), valence (red), and mixed (green) excited states of the benzene dimer at the equilibrium geometry of (a) the excimer and (b) the cation. The mixed Rydberg-valence states are below the cutoff for obvious Rydberg states (e.g., $\Delta\langle R^2\rangle$ < 43 au^2), however, they are more diffuse than pure valence states, $\Delta\langle R^2\rangle$ < 15 au^2.

6.87 eV in direct absorption experiments of jet-cooled benzene[48] (7.52 eV in our calculations). The resulting E_{1u} excimer state has been deemed responsible for the excimer absorption band,[24] even though it is symmetry-forbidden. Note that the shape of the PES of this excimer state is different in CASPT2 (ref 36.) and EOM-CCSD (ref 37 and this work) calculations, for example, the

dx.doi.org/10.1021/jp209190e |J. Phys. Chem. A 2012, 116, 653–662

Table 1. Excitation Energies (E_{ex}, eV) and Changes in $\langle R^2 \rangle$ (au^2) Values for the Excited Singlet States of the Dimer at the Excimer's Equilibrium Geometry (D_{6h} Geometry, Using D_{2h} Point Group Labels)

state	E_{ex}	$\Delta\langle R^2\rangle$	state	E_{ex}	$\Delta\langle R^2\rangle$
$1A_g$	7.03	52	$2A_u$	6.43	41
$2A_g$	7.08	53	$3A_u$	7.77	54
$1B_{1g}$	7.08	53	$1B_{1u}$	6.24	40
$2B_{1g}$	7.18	55	$2B_{1u}$	6.33	40
$1B_{2g}$	5.43	3	$3B_{1u}$	7.77	54
$2B_{2g}$	5.71	4	$1B_{2u}$	5.26	3
$3B_{2g}$	5.91	31	$2B_{2u}$	6.50	44
$4B_{2g}$	6.81	44	$3B_{2u}$	7.39	32
$5B_{2g}$	6.81	45	$4B_{2u}$	7.43	26
$6B_{2g}$	7.38	32	$5B_{2u}$	7.65	29
$1B_{3g}$	4.39	2	$6B_{2u}$	7.80	20
$2B_{3g}$	5.71	4	$1B_{3u}$	6.50	44
$3B_{3g}$	5.91	31	$2B_{3u}$	6.85	11
$4B_{3g}$	6.78	43	$3B_{3u}$	7.39	32
$5B_{3g}$	6.81	44	$4B_{3u}$	7.41	20
$6B_{3g}$	7.38	32	$5B_{3u}$	7.65	29
$1A_u$	6.33	40	$6B_{3u}$	7.80	20

Table 2. Excitation Energies (E_{ex}, eV) and Changes in $\langle R^2 \rangle$ (au^2) Values for the Excited Singlet States of the Dimer at the Cation's Equilibrium Geometry (C_{2h} Symmetry)

state	E_{ex}	$\Delta\langle R^2\rangle$	state	E_{ex}	$\Delta\langle R^2\rangle$
$1A_g$	4.91	2	$1A_u$	6.57	38
$2A_g$	6.30	26	$2A_u$	6.64	40
$3A_g$	6.39	12	$3A_u$	6.73	14
$4A_g$	7.03	45	$4A_u$	6.82	39
$5A_g$	7.18	47	$5A_u$	7.40	18
$6A_g$	7.23	47	$6A_u$	7.48	16
$7A_g$	7.32	40	$7A_u$	7.65	31
$8A_g$	7.60	37	$8A_u$	7.88	25
$9A_g$	7.86	16	$9A_u$	7.97	42
$10A_g$	8.05	40	$10A_u$	8.02	39
$1B_g$	6.06	4	$1B_u$	5.23	3
$2B_g$	6.12	32	$2B_u$	6.49	39
$3B_g$	6.43	6	$3B_u$	6.69	44
$4B_g$	7.08	46	$4B_u$	6.75	36
$5B_g$	7.24	48	$5B_u$	7.41	14
$6B_g$	7.31	44	$6B_u$	7.43	25
$7B_g$	7.40	48	$7B_u$	7.57	35
$8B_g$	7.54	34	$8B_u$	7.87	42
$9B_g$	7.96	33	$9B_u$	7.89	21
			$10B_u$	7.99	40

CASPT2 curve has a hump, which is probably due to discontinuity in the active space or an intruder state.

This simple picture, however, is an oversimplification, as the excited-states manifold is much more complicated due to the multiple Rydberg states and avoided crossings. Figure 4 shows a scan along the interfragment distance R of the dense manifold of excited states that are below the calculated ionization threshold

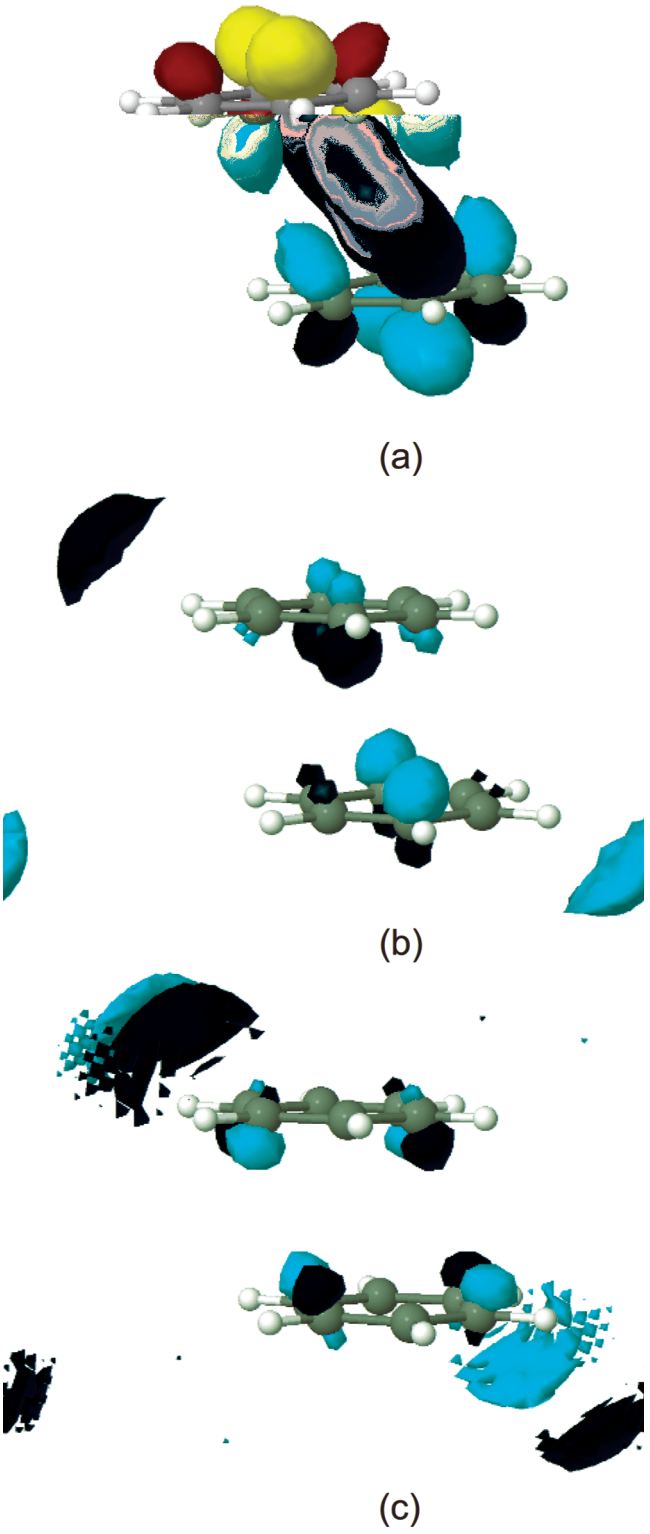

Figure 7. Virtual orbitals giving rise to the two brightest excited states ($5B_u$ and $6B_u$) of the x-displaced sandwich excimer (see text). The 6-31+G(d) basis set was used in the calculation and the isosurface in the plot was 0.032.

(7.89 eV) at the equilibrium geometry of the excimer. At this level of theory, the lowest excimer state lies 4.39 eV above the ground state and is well separated from the higher-energy states. Allowing for structural relaxation of the excimer by geometry

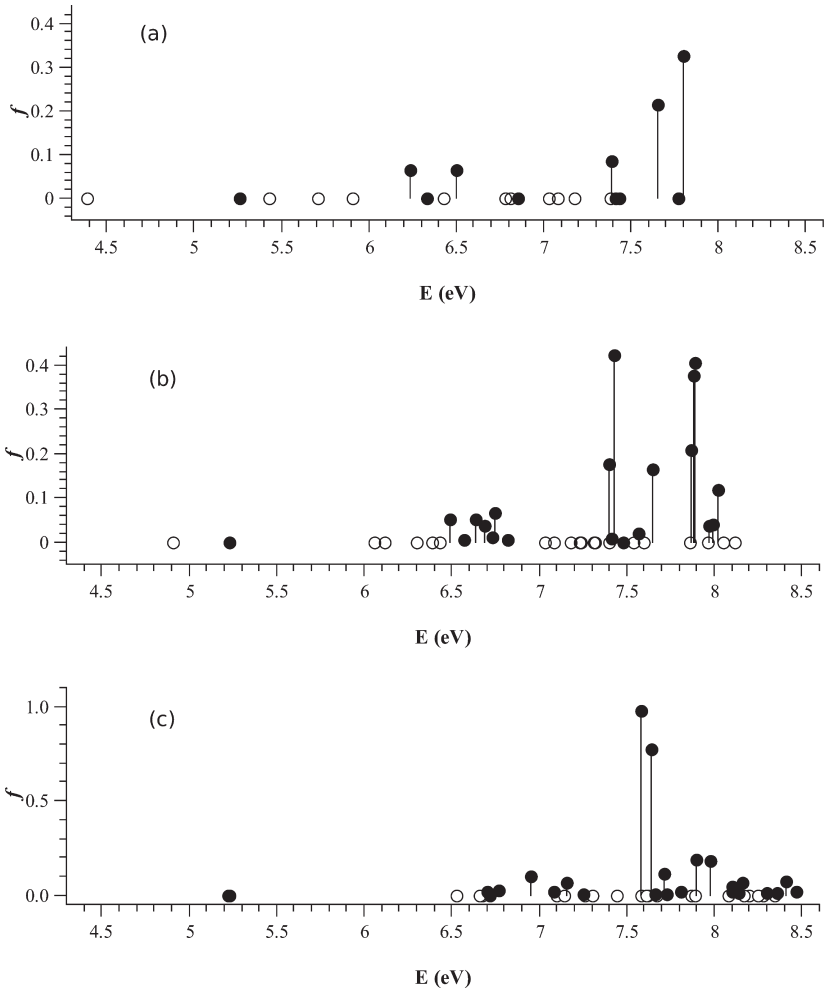

Figure 8. Absorption of the ground-state dimer at the equilibrium geometries of the excimer (a), cation (b), and the parallel-displaced ground-state structure (c). Empty circles denote forbidden transitions, whereas filled circles stand for allowed ones.

optimization of this state brings it slightly down in energy, to 4.34 eV. Experimentally, it is observed at 3.94 eV,[52] in fluorescence emission of liquid benzene.

Figure 5 shows a pruned manifold focusing on the states that are relevant to our discussion and omitting the rest of the states for clarity. The figure is analogous to the cartoon picture (Figure 2) except that it also includes a few extra features. The first important difference is the curves resulting from the degenerate Rydberg state in the monomer at 6.85 eV. In the D_{2h} point group, this state splits into B_{2g} and B_{3g} states, and these give rise to two pairs of degenerate states in the dimer ($2B_{2g}$ + $2B_{3g}$ and $2B_{2u}$ + $1B_{3u}$), the latter pair of states being the higher energy curve. Note that the lowest three B_{2g} states can interact through curve crossings such that several relaxation channels could open up depending on the couplings between these states. The second important feature is the uppermost curve ($4B_{2u}$ and $4B_{3u}$ states). These were included because they cross the $3B_{2u}$ + $3B_{3u}$ curves (which correspond to the top pair of dimer states in Figure 2, one of which is responsible for the absorption band of the excimer). This will be further discussed in section 3.3.

Now we turn to the *x*-displaced sandwich structure (i.e., equilibrium structure of the dimer cation). The orbitals at this geometry are very similar to the ones of the D_{6h} sandwich structure, the only noticeable difference being the breaking of the degeneracy of the π-system as a result of the reduced symmetry, which leads to splitting of the states that were degenerate at D_{6h}.

To qualitatively assign states characters (e.g., Rydberg vs valence), we use changes in the $\langle R^2 \rangle$ values of the excited states (relative to the ground state), $\Delta\langle R^2 \rangle$ (see ref 53.). We consider the states that exhibit a change in $\langle R^2 \rangle$ larger than 12 Å^2 (≈43 au^2) to be of a Rydberg character, using the same cutoffs as in ref 53. We consider states with $\Delta\langle R^2 \rangle$ < 15 au^2 to be of purely valence, and the states with 15 ≤ $\Delta\langle R^2 \rangle$ < 43 au^2 of mixed Rydberg-valence character.

Figure 6 shows an energy level diagram of the benzene dimer at the excimer and the cation geometries. The states are color-coded according to their $\Delta\langle R^2 \rangle$ values in Tables 1 and 2. Even though the two structures are very similar, the excited states ordering changes considerably. This is because splitting between excimer-like pairs of states depends on the overlap between the respective MOs, which is strongly distance-dependent. In panel (a), we have labeled only the states that are depicted in Figure 5. The most important state is $4B_{2u}$, which is responsible for the excimer's absorption. In panel (b), we give labels only for several states of interest. The lowest five of these ($1A_g$, $1B_u$, $1B_g$, $3A_g$, and $3B_g$) are clearly valence states and correspond to excitations from the highest two occupied, to the lowest two unoccupied π-orbitals. This can be mapped to a HOMO−LUMO excitation

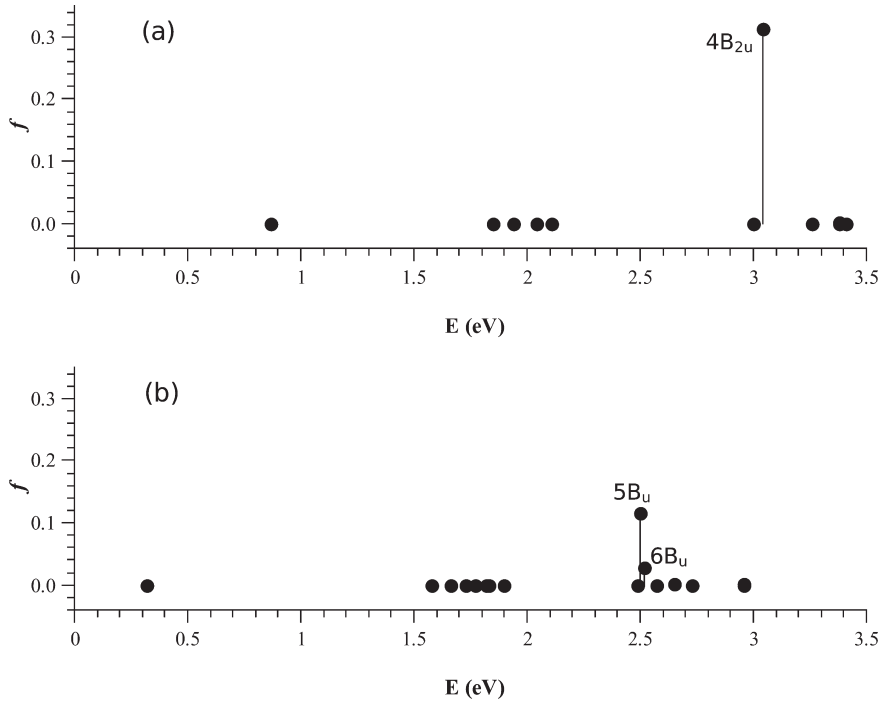

Figure 9. Absorption of the excimer (the 1^1B_{1g} state in D_{6h}, or 1^1B_{3g} in D_{2h}) at the equilibrium excimer (slightly distorted to D_{2h}) geometry (a) and the equilibrium cation geometry (b). Only symmetry-allowed transitions are shown.

in the sandwich structure in a minimal basis set, except that here (in the *x*-displaced sandwich structure) the π-orbitals are no longer exactly degenerate, but rather are, very close in energy. The other two states of interest ($5B_u$ and $6B_u$, which are the states that carry large oscillator strength for the excimer absorption and correlate with the $4B_{2u}$ state at the excimer geometry, panel (a)) lie higher in energy and are immersed in the dense manifold of states. They result from excitations to π-like orbitals which are strongly mixed with Rydberg type orbitals and give rise to the absorption of the excimer in the x-displaced structure (see Figure 9b). The $5B_u$ state would correspond to HOMO-1 to LUMO excitation in a symmetric sandwich structure (in a minimal basis set), but in a realistic basis set, it is strongly mixed with an excitation to a low-lying Rydberg orbital. The excitation is almost an equal mix of two excitations to the orbitals labeled as (a) and (b) in Figure 7. Note the valence-like π character of (a) and the mixed (π-Rydberg) character of (b). This mixing gives rise to a larger $\Delta\langle R^2\rangle$ value (=14 au^2) for the $5B_u$ state compared to pure valence states. The $6B_u$ state, on the other hand, features an excitation to an even more strongly mixed valence-Rydberg state, which, as expected, has a relatively large $\Delta\langle R^2\rangle$ value (=25 au^2). Again, similarly to the $5B_u$ state, it is composed of two excitations, including an excitation to orbital (b) in Figure 7, however, the main excitation is to orbital (c), with an amplitude of 0.42, as opposed to an amplitude of 0.26 to orbital (b).

3.2. Absorption of the Ground-State Benzene Dimer. Figure 8 shows the stick absorption spectrum of the ground-state dimer at different geometries. As one can see, there are two groups of states that have nonzero oscillator strengths, one clustered around 6.5 eV, and then several states close to the ionization threshold (between 7.7 and 8 eV). The spectra are qualitatively similar, showing a relatively small apparent effect of the structure, although the excitation energies of individual states (many of them being dark) change quite considerably, as illustrated in Figure 8. The excitation to the lowest excimer state is symmetry-forbidden by parity at D_{6h}, D_{2h}, and C_{2h}. Thus, small nuclear displacements are not expected to lead to a significant gain in the oscillator strength.

3.3. Absorption Spectrum of the Excimer. Figure 9 shows the calculated absorption spectrum (symmetry-allowed transitions in D_{2h}, some of which may be forbidden in D_{6h}) of the excimer, that is, transitions from the lowest excited state, 1^1B_{3g} (1^1B_{1g} at D_{6h}), of the sandwich-shaped dimer. The spectrum features a strong $1B_{3g} \rightarrow 4B_{2u}$ ($1B_{1g} \rightarrow E_{1u}$ in D_{6h}) absorption (see Figure 5) at 3.04 eV, about a half eV higher than the experimentally observed peak at 2.48 eV.[14] In a larger basis set we would expect the calculated peak to shift to a lower energy based on our observations that larger basis set calculations predict a larger stabilization of the higher energy excited states compared to the lowest excimer state, since higher energy states are usually either Rydberg or strongly mixed valence-Rydberg types of states, whereas the lowest excimer state shows a much more valence-like character. However, increasing the basis set size to 6-311++G(d,p) has a very small effect on the absorption energy, reducing it to 2.99 eV, close to the value of 2.89 eV (from linear response CCSD calculations), reported in ref 37. The latter study also noted the relative insensitivity of the absorption energy to the basis set. For example, switching to aug-cc-pVQZ from aug-cc-pVDZ increases the absorption energy by only 0.07 eV in RI-CC2 calculations. In the same paper, the effect of perturbative triples is found to be relatively small (CCSDR(3) giving an absorption energy of 3.00 eV, as opposed to 2.89 eV from CCSD). The combined effect of perturbative triples correction and extrapolation to a larger basis set brings the absorption energy closer to the CCSD/aug-cc-pVDZ value.[37] We find, however, that expanding the basis set has a more pronounced effect on the oscillator strength of this absorption, reducing it to 0.265 au (6-311++G(d,p)) from 0.313 au (6-31+G(d)). Overall, given the broad nature of the

dx.doi.org/10.1021/jp209190e |*J. Phys. Chem. A* 2012, 116, 653–662

experimental excimer absorption spectrum, it is unrealistic to expect a perfect agreement between vertical excitation energy and the absorption maximum.

A closer look at the $3B_{2u}$ and $4B_{2u}$ states around the equilibrium geometry of the excimer reveals that they are derived from the same excitations, but with different signs. At this geometry, the $4B_{2u}$ state (formed by $x \rightarrow y + x' \rightarrow y'$ excitation, where x and x' are the HOMO orbitals, b_{3g} and b_{2g}, respectively, while y and y' are orbitals composed of a strong mix of Rydberg orbitals with the virtual b_{1u} and a_u orbitals, respectively, in Figure 1) is only slightly higher in energy than the $3B_{2u}$ one ($x \rightarrow y - x' \rightarrow y'$ excitation), while at larger R, the former $4B_{2u}$ state becomes $3B_{2u}$. It is straightforward to show that in a three-center D_{3h} Hückel system, a calculation of oscillator strengths predicts that one of these states will be bright, while the other will be dark. This is what we observe in our case; the excitation to the $4B_{2u}$ state at the (slightly distorted) equilibrium geometry of the excimer is the bright one, with an oscillator strength of 0.313 au. One would not expect noticeable changes in the oscillator strength for the excimer emission transition ($1B_{1g} \rightarrow 1A_{1g}$ in D_{6h}, or $1B_{3g} \rightarrow 1A_g$ in D_{2h}) due to small nuclear displacements, because the excimer state is not degenerate and the transition is parity-forbidden not only in D_{6h} but also in the lower symmetry D_{2h} and C_{2h} point groups. This could explain why the experimentally observed excimer absorption is brighter than the excimer emission, even though both transitions are symmetry-forbidden at the equilibrium geometry of the excimer (D_{6h}).

The absorption spectrum of the excimer at the geometry of the cation (Figure 9b) is drastically different from the symmetric structure. The displaced excimer absorbs at much lower energies (0.5 eV) relative to the symmetric geometry, and this seems to be mostly due to the fact that the lowest excimer state in the x-displaced sandwich lies much higher in energy (also about 0.5 eV) with respect to the sandwich structure. This strong variation of absorption with structure is consistent with the experimentally observed broad excimer absorption.

4. CONCLUSIONS

We investigated the electronically excited states of the benzene dimer using EOM-CCSD. The excited-state manifold is very dense and contains numerous interacting states. The lowest valence states are derived from the HOMO−LUMO transitions, whereas the higher-energy manifold (above 6 eV) is dominated by Rydberg states. Most importantly, at higher energies some Rydberg states become mixed with valence transitions giving rise to mixed Rydberg-valence states.

This complexity can be tackled by the EOM-EE-CC method, which does not involve active space selection, state-averaging, and correctly reproduces electronic degeneracies, which are prominently present in this high-symmetry system.

Our calculations of the excimer state structure and excitation energy are in agreement with previous studies, for example, EOM-EE-CCSD/6-31+G* geometry optimization of the lowest singlet state of the dimer (1^1B_{1g}) yields D_{6h} sandwich structure with an interfragment distance of 3.15 Å. The estimated vertical energy gap between the relaxed excimer structure and the ground state is 4.34 eV.

We identify the target state responsible for the excimer absorption as the E_{1u} state at 3.04 eV (relative to the excimer, 1^1B_{1g}), which has a mixed Rydberg-valence character. Calculations of oscillator strengths corresponding to the transitions between the excimer (which is an excited state of the dimer) and other excited states clearly reveal one bright transition. At D_{6h}, the symmetry of this target state is E_{1u}, which makes this electronic transition symmetry-forbidden, however, tiny geometric displacements (to D_{2h}) that have negligible effect on the excitation energy split this degenerate state into the dark $4B_{3u}$ and bright $4B_{2u}$ components (f_l = 0.3 au). This is the key to explaining the puzzling strong absorption band of the benzene excimer assigned to a transition which is symmetry-forbidden from a group theoretical perspective. That is, the absorption is due to symmetry lowering as a result of molecular vibrations, rather than intensity borrowing from other states via vibronic coupling. While this instantaneous symmetry lowering strongly enhances the otherwise symmetry-forbidden excimer absorption, it does not have a significant effect on the excimer emission transition ($1B_{1g} \rightarrow 1A_{1g}$ in D_{6h}, or $1B_{3g} \rightarrow 1A_g$ in D_{2h}) because this transition is symmetry forbidden by parity, which explains the relative cross sections for the two processes.

■ ASSOCIATED CONTENT

Supporting Information. Relevant Cartesian geometries, energies, and oscillator strengths are provided. This material is available free of charge via the Internet at http://pubs.acs.org.

■ ACKNOWLEDGMENT

This work is conducted under the auspices of the *iOpenShell* Center for Computational Studies of Electronic Structure and Spectroscopy of Open-Shell and Electronically Excited Species supported by the National Science Foundation through the CRIF:CRF CHE-0625419 + 0624602 + 0625237 and CHE-0951634 Grants. We are thankful to Dr. Piotr Pieniazek, Prof. Lyudmila Slipchenko, and Prof. Stephen Bradforth for valuable comments.

■ REFERENCES

(1) Sinnokrot, M. O.; Sherrill, C. D. *J. Phys. Chem. A* **2004**, *108*, 10200.
(2) Cundall, R. B.; Robinson, D. A. *J. Chem. Soc., Faraday Trans. 2* **1972**, 1133.
(3) Hirayama, F.; Lipski, S. *J. Chem. Phys.* **1969**, *51*, 1939.
(4) Rayleigh, Lord *Proc. R. Soc. A* **1927**, *116*, 702.
(5) Hopfield, J. J. *Phys. Rev.* **1930**, *35*, 1133.
(6) Hopfield, J. J. *Astrophys. J.* **1930**, *72*, 133.
(7) Birks, J. B. *Rep. Prog. Phys.* **1975**, *38*, 903.
(8) Hirayama, F. *J. Chem. Phys.* **1965**, *42*, 3163.
(9) Eisinger, J.; Gueron, M.; Shulman, R. G.; Yamane, T. *Proc. Natl. Acad. Sci. U.S.A.* **1966**, *55*, 1015.
(10) Kohler, B. *J. Phys. Chem. Lett.* **2010**, *1*, 2047.
(11) Middleton, C. T.; de La Harpe, K.; Su, C.; Law, Y. K.; Crespo-Hernández, C. E.; Kohler, B. *Annu. Rev. Phys. Chem.* **2009**, *60*, 217.
(12) Förster, T. H.; Kasper, K. *Z. Phys. Chem.* **1954**, *1*, 275.
(13) Waldman, A.; Ruhman, S. *Chem. Phys. Lett.* **1993**, *215*, 470.
(14) Hirata, T.; Ikeda, H.; Saigusa, H. *J. Phys. Chem. A* **1999**, *103*, 1014.
(15) Saigusa, H.; Morohoshi, M.; Tsuchiya, S. *J. Phys. Chem. A* **2001**, *105*, 7334.
(16) Hopkins, J. B.; Powers, D. E.; Smalley, R. E. *J. Phys. Chem.* **1981**, *85*, 3739.
(17) Law, K.; Schauer, M.; Bernstein, E. R. *J. Chem. Phys.* **1984**, *81*, 4871.
(18) Nakashima, N.; Sumitani, M.; Ohmine, I.; Yoshihara, K. *J. Chem. Phys.* **1980**, *72*, 2226.

(19) Richards, J. T.; Thomas, J. K. *Chem. Phys. Lett.* **1970**, *5*, 527.
(20) Cooper, R.; Thomas, J. K. *J. Chem. Phys.* **1968**, *48*, 5097.
(21) Bonneau, R.; Josset-Dubien, R.; Bensasson, R. *Chem. Phys. Lett.* **1969**, *3*, 353.
(22) Shinohara, H.; Nishi, N. *J. Chem. Phys.* **1989**, *91*, 6743.
(23) Katoh, R.; Katoh, E.; Nakashima, N.; Yuuki, M.; Kotani, M. *J. Phys. Chem. A* **1997**, *101*, 7725.
(24) Birks, J. B. *Chem. Phys. Lett.* **1968**, *1*, 625.
(25) Bensasson, R. V.; Richards, J. T.; Thomas, J. K. *Chem. Phys. Lett.* **1971**, *9*, 13.
(26) Vala, M. T.; Hillier, I. H.; Rice, S. A.; Jortner, J. *J. Chem. Phys.* **1966**, *44*, 23.
(27) East, A. L. L.; Lim, E. C. *J. Chem. Phys.* **2000**, *113*, 8981.
(28) Levchenko, S.; Reisler, H.; Krylov, A.; Gessner, O.; Stolow, A.; Shi, H.; East, A. L. L. *J. Chem. Phys.* **2006**, *125*, 084301.
(29) Kozak, C. R.; Kistler, K. A.; Lu, Z.; Matsika, S. *J. Phys. Chem. B* **2010**, *114*, 1674.
(30) Golubeva, A. A.; Krylov, A. I. *Phys. Chem. Chem. Phys.* **2009**, *11*, 1303.
(31) Bravaya, K. B.; Kostko, O.; Ahmed, M.; Krylov, A. I. *Phys. Chem. Chem. Phys.* **2010**, *12*, 2292.
(32) Birks, J. B. *Photophysics of Aromatic Molecules*; John Wiley & Sons Ltd: New York, 1970.
(33) Chesnut, D. B.; Fritchie, C. J.; Simmons, H. E. *J. Chem. Phys.* **1965**, *42*, 1127.
(34) Srinivasan, B. N.; Russell, J. V.; McGlynn, S. P. *J. Chem. Phys.* **1968**, *48*, 1931.
(35) Amicangelo, J. C. *J. Phys. Chem. A* **2006**, *109*, 9174.
(36) Rocha-Rinza, T.; Vico, L. De; Veryazov, V.; Roos, B. O. *Chem. Phys. Lett.* **2006**, *426*, 268272.
(37) Rocha-Rinza, T.; Christiansen, O. *Chem. Phys. Lett.* **2009**, *482*, 4449.
(38) Krylov, A. I. *Annu. Rev. Phys. Chem.* **2008**, *59*, 433.
(39) Mozhayskiy, V. A.; Babikov, D.; Krylov, A. I. *J. Chem. Phys.* **2006**, *124*, 224309.
(40) Mozhayskiy, V. A.; Krylov, A. I. *Mol. Phys.* **2009**, *107*, 929.
(41) Pieniazek, P. A.; Krylov, A. I.; Bradforth, S. E. *J. Chem. Phys.* **2007**, *127*, 044317.
(42) Savee, J. D.; Mozhayskiy, V. A.; Mann, J. E.; Krylov, A. I.; Continetti, R. E. *Science* **2008**, *321*, 826.
(43) Mozhayskiy, V. A.; Savee, J. D.; Mann, J. E.; Continetti, R. E.; Krylov, A. I. *J. Phys. Chem. A* **2008**, *112*, 12345.
(44) Gauss, J.; Stanton, J. F. *J. Phys. Chem. A* **2000**, *104*, 2865.
(45) Stanton, J. F.; Bartlett, R. J. *J. Chem. Phys.* **1993**, *98*, 7029.
(46) Y. Shao; Molnar, L. F.; Jung, Y.; Kussmann, J.; Ochsenfeld, C.; Brown, S.; Gilbert, A. T. B.; Slipchenko, L. V.; Levchenko, S. V.; O'Neil, D. P.; Distasio, R. A., Jr; Lochan, R. C.; Wang, T.; Beran, G. J. O.; Besley, N. A.; Herbert, J. M.; Lin, C. Y.; Van Voorhis, T.; Chien, S. H.; Sodt, A.; Steele, R. P.; Rassolov, V. A.; Maslen, P.; Korambath, P. P.; Adamson, R. D.; Austin, B.; Baker, J.; Bird, E. F. C.; Daschel, H.; Doerksen, R. J.; Dreuw, A.; Dunietz, B. D.; Dutoi, A. D.; Furlani, T. R.; Gwaltney, S. R.; Heyden, A.; Hirata, S.; Hsu, C.-P.; Kedziora, G. S.; Khalliulin, R. Z.; Klunziger, P.; Lee, A. M.; Liang, W. Z.; Lotan, I.; Nair, N.; Peters, B.; Proynov, E. I.; Pieniazek, P. A.; Rhee, Y. M.; Ritchie, J.; Rosta, E.; Sherrill, C. D.; Simmonett, A. C.; Subotnik, J. E.; Woodcock, H. L., III; Zhang, W.; Bell, A. T.; Chakraborty, A. K.; Chipman, D. M.; Keil, F. J.; Warshel, A.; Herhe, W. J.; Schaefer, H. F., III; Kong, J.; Krylov, A. I.; Gill, P. M. W.; Head-Gordon, M. *Phys. Chem. Chem. Phys.* **2006**, *8*, 3172.
(47) Lassetre, E. N.; Skerbele, A.; Dillon, M. A.; Roos, K. J. *J. Chem. Phys.* **1968**, *48*, 5066.
(48) Hiraya, A.; Shobatake, K. *J. Chem. Phys.* **1991**, *94*, 7700.
(49) Gregory, T. A.; Helman, W. P. *J. Chem. Phys.* **1972**, *56*, 377.
(50) Ernstberger, B. *Ph.D. Thesis*, Technische Universität München, 1991.
(51) Radloff, W.; Freudenberg, Th.; Ritze, H.-H.; Stert, V.; Noack, F.; Hertel, I. V. *Chem. Phys. Lett.* **1996**, *261*, 301.
(52) Azumi, T.; McGlynn, S. P. *J. Chem. Phys.* **1964**, *41*, 3131.
(53) Reisler, H.; Krylov, A. I. *Int. Rev. Phys. Chem.* **2009**, *28*, 267.